International Journal of Multidisciplinary and Current Research ISSN: 2321-3124
Research Article Available at: https://ijmcr.com

QSAR, human hepatocellular carcinoma anticancer screening, docking studies and *in silico* prediction of some *N*-(substituted)-9-alkyl-1- substituted-9*H*-β-carboline-3-carboxamide derivatives

Abdelrahman Hassan Ahmed[1*], Amna Bint Wahab Elrashid Mohammed Hussien[2], Ahmed Elsadig Mohammed Saeed[3]

[1]Department of Chemical Engineering, College of Engineering, Karary University, 12304, Khartoum, Sudan
[2]Colege of Produed Animal, Sudan University of Science and Technology, 407, Khartoum, Sudan
[3]Department of Chemistry, College of Science, Sudan University of Science and Technology, 407, Khartoum, Sudan

Received 01 Mar 2026, Accepted 18 Mar 2026, Available online 20 Mar 2026, **Vol.14, No.2 (Mar/Apr 2026)**

Abstract

A quantitative structure activity relationship (QSAR) model for a series of β- carboline derivatives having human hepatocellular carcinoma inhibitory activities as effective anticancer agents was developed by the multiple linear regressions (MLR) method. In this study, the compounds were used in the model development were divided into a set of fifteen compounds as training set and set of four compounds as test set. A model with high prediction ability and high correlation coefficients was obtained. This model showed r = 0.9760, r2 = 0.9530 and Q2 = 0.903, the QSAR model was also employed to predict the experimental compounds in an external test set, and to predict the activity of a new designed set of N-(2-amino-2-substitutedethyl)-9-(substituted)-6 substituted-1- substituted- 9H-β- carboline-3 carboxamide derivatives (M1-M50), result showed that compound M30 has the most promising inhibition activity (pIC50 = 11.6455) against human hepatocellular carcinoma cell line (Bel7402). Besides, the model showed good correlative and predictive ability. The Docking studies show that compound M12 and M19 have the highest binding scores -9.7602 and -9.1456 kcal/mol respectively.

Keywords: *Qsar, Molecular Docking, Hepatocellular Carcinoma, B-Carboline Compounds*

1. Introduction

The World Health Organization reports reveal that cancer is a real public health problem because around 10 million deaths were recorded in 2020. According to the same source, 19 million new cases appear in year 2020. This alarming increase of new patients with cancer entails health sectors to take proactive measures to cease this upsurge. The numbers associated to this pathology situate liver cancer at the third position (8.3%) after lung (18%) and colorectum (9.4%) (Ferlay et al, 2020; Taïbi et al, 2019).

Liver cancer remains a global health challenge and its incidence is growing worldwide (Llovet et al, 2021). It is estimated that, by 2030, over one million sufferers will be died by liver cancer (Villanueva, 2019). Hepatocellular carcinoma (HCC) as the most common form of liver cancer accounts for around 90% of cases (Man et al, 2021; Anwanwan et al, 2020). Despite the great advances made in the chemotherapeutic management of cancer patients, discovering novel efficient anticancer agents, selective on cancerous and less toxic to normal cells, is still one of the hottest areas in medicinal chemistry research (Omran et al, 2019).

*Correspondant Author's ORCID ID: 0000-0000-0000-0000
DOI: https://doi.org/10.14741/ijmcr/v.14.2.11

HCC most-commonly develops in people associated with liver disease, particularly in people with chronic hepatitis B and C. Symptoms often don't appear in the early stages but in later stage, symptoms include weight loss, upper abdominal pain or yellowing of the skin (Jaundice)(Suganya and Anuradha, 2019; El-Miligy et al, 2018).

Quantitative structure-activity relationship (QSAR) model correlates the biological activity of molecules with its structural features represented as multiple molecular descriptors (MDs), which has been widely used in many fields (Li et al, 2021). The advantages of having QSAR models for drug design are numerous: reduction of the time spent during the discovery phase, reduction of economic and material resources required (Martinez et al, 2019). The molecular docking technology is a research method used in drug discovery and screening for new drug candidates (Abdolmaleki et al, 2017). Based on the "key and lock" concept, the active sites between the ligand and the target protein can be identified. The most suitable binding conformation and combination of the ligand and the receptor can be found (Fischer, 1894; Li et al, 2019).

DNA has long been proven to be the most important target in cancer therapy. Generally, DNA interactive drugs

include DNA-alkylating agents, DNA intercalators, and DNA groove binders (Almaqwashi et al, 2019).

In accompany of this fact the study built a quantitative structure activity relationship (QSAR) model and used to predict the biological activity of a set of designed β-carboline derivatives and dock them as DNA targeting anti hepatocellular carcinoma agents, searching for new leads compounds.

2. Experimental

2.1. QSAR studies

A total of nineteen N-(substituted)-9-alkyl-1-substituted-9H-β-carboline-3- carboxamide derivatives reported by (Guan et al, 2006) were used in QSAR study (table 1). They synthesized a number of N-(substituted)-9-alkyl-1-substituted-9H-β-carboline-3-carboxamide derivatives and reported their in vitro cytotoxic activity against eight human cancer cell lines, Bel7402, Hela, C6, Lovo, PLA801, BGC823, HFL-1 and VSMC, respectively, including human hepatocellular carcinoma cell line (Bel7402). ACD/lab free software (Copyright 1994-2013, ACD/Labs Release 2012, File Version 14.01, Build 65895, 17 Sep 2013) was used for drawing series of the studied compounds.

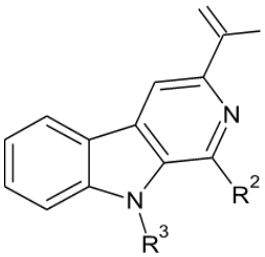

Table 1: Anticancer activities and structures of *N*-(substituted)-9-alkyl-1-substituted- 9*H*-β-carboline-3-carboxamide derivatives reported by (Guan *et al*, 2006)

Compound ID	R1	R2	R3	IC50	pIC50
1	-(CH2)2NH2	0	-C2H5	0.016	7.7959
2	-(CH2)2NH2	0	n-C4H9	0.0298	7.5258
3	-(CH2)2NH2	0	-CH2C6H5	0.0056	8.2518
4	-(CH2)2NH2	0	-CH2C6F5	0.0336	7.4737
5	-(CH2)2NH2	H	0	0.0138	7.8601
6	-(CH2)2NH2	H	-C2H5	0.0293	7.5331
7	-(CH2)2NH2	H	-CH2C6H5	0.00714	8.1463
8	-(CH2)2OH	0	0	0.0335	7.475
9	-(CH2)2OH	0	-C2H5	0.123	6.9101
10	-(CH2)2OH	0	n-C4H9	0.174	6.7595
11	-(CH2)2OH	0	-CH2C6F5	0.109	6.9626
12	-(CH2)2OH	H	0	0.108	6.9666
13	-(CH2)2OH	H	-C2H5	0.0328	7.4841
14	-(CH2)2OH	H	n-C4H9	0.121	6.9172
15	-(CH2)2OH	H	-CH2C6H5	0.0268	7.5719
16	-(CH2)6NH2	0	-CH2C6F5	0.418	6.3788
17	-(CH2)6NH2	H	0	0.422	6.3747
18	-(CH2)6NH2	H	-C2H5	0.235	6.6289
19	-(CH2)6NH2	H	-CH2C6H5	0.0191	7.719

Table 2: Values of mixed (2D & 3D) descriptors calculated for development of QSAR model

ID	Log P(O/W)	E_ele	BCUT_SLOGP_0	CASA+	a_aro	vsurf_EDmin3
1	2.0395	7.4319	-2.7731	849.922	13	-2.6461
2	3.0955	7.4296	-2.7731	840.753	13	-2.6753
3	3.4865	12.4434	-2.7731	1462.07	19	-2.8236
4	4.2395	8.2199	-2.7731	1269.31	19	-2.7969
5	1.4405	7.8793	-2.7731	984.008	13	-2.4341
6	1.7815	7.9195	-2.7731	885.423	13	-2.6196
7	3.2285	12.7963	-2.7731	1488.14	19	-2.805
8	1.9205	5.8673	-2.6741	773.232	13	-2.503
9	2.2615	5.8132	-2.6741	703.107	13	-2.6417
10	3.3175	5.9181	-2.6741	679	13	-2.5246
11	4.4615	5.2764	-2.6741	1111.11	19	-2.8122
12	1.6625	6.2653	-2.6739	814.839	13	-2.4153
13	2.0035	6.2738	-2.6739	752.051	13	-2.6116
14	3.0595	6.2429	-2.6739	737.956	13	-2.6509
15	3.4505	12.6714	-2.6739	1274.3	19	-2.953
16	5.2545	4.7702	-2.6944	1438.37	19	-2.7777
17	3.2085	0.6512	-2.6944	934.183	13	-2.4424
18	3.5495	0.7246	-2.6944	835.642	13	-2.4745
19	4.9965	5.5729	-2.6944	1462.5	19	-2.901

Table 3: Values of (2D) descriptors calculated for development of QSAR model

ID	Log P(O/W)	PC-	Q_PC+	GCUT_SLOGP_3	desity
1	2.0395	-3.964	3.964	2.4747	0.7099
2	3.0955	-3.964	3.964	2.3722	0.6957
3	3.4865	-4.858	4.857	2.3722	0.7056
4	4.2395	-5.057	5.057	2.3242	0.8561
5	1.4405	-3.964	3.964	2.2222	0.7279
6	1.7815	-3.964	3.964	2.2372	0.7183
7	3.2285	-4.858	4.857	2.4422	0.7122
8	1.9205	-3.654	3.654	2.2372	0.7323
9	2.2615	-3.654	3.654	2.4772	0.7229
10	3.3175	-3.654	3.654	2.32.2	0.7071
11	4.4615	-4.748	4.747	2.3272	0.8682
12	1.6625	-3.654	7.227	2.2223	0.7429
13	2.0035	-3.654	7.227	2.24.3	0.7323
14	3.0595	-3.654	3.654	2.4427	0.7146
15	3.4505	-4.548	4.547	2.4234	0.7234
16	5.2545	-4.858	4.857	2.3372	0.6844
17	3.2085	-3.964	3.964	2.4222	0.6957
18	3.5495	-3.964	3.964	2.4277	0.6898
19	4.9965	-4.858	4.857	2.324.	0.689

Table 4: Values of (3D) descriptors calculated for development of QSAR model

ID	Log P(O/W)	E_ele	PM3_HOMO	VSA	vsurf_DW3
1	2.0395	7.4319	-8.6411	334.84	2.4242
2	3.0955	7.4296	-8.4715	376.429	2.4242
3	3.4865	12.4434	-8.4616	396.996	2.2222
4	4.2395	8.2199	-8.7159	412.57	2.4242
5	1.4405	7.8793	-8.7677	299.446	0.5
6	1.7815	7.9195	-8.7391	318.534	2.4242
7	3.2285	12.7963	-8.5852	382.496	2.3222
8	1.9205	5.8673	-8.7029	306.838	0.5
9	2.2615	5.8132	-8.6857	329.123	0.5
10	3.3175	5.9181	-8.7038	367.666	1
11	4.4615	5.2764	-8.7687	405.471	0.7071
12	1.6625	6.2653	-8.7923	291.582	0.5
13	2.0035	6.2738	-8.7623	313.039	0.7071
14	3.0595	6.2429	-8.6504	354.513	0.7071
15	3.4505	12.6714	-8.6044	376.589	0.866
16	5.2545	4.7702	-8.4587	475.204	1.2247
17	3.2085	0.6512	-8.749	380.402	0.5
18	3.5495	0.7246	-8.731	398.692	0.5
19	4.9965	5.5729	-8.5603	464.278	0.5

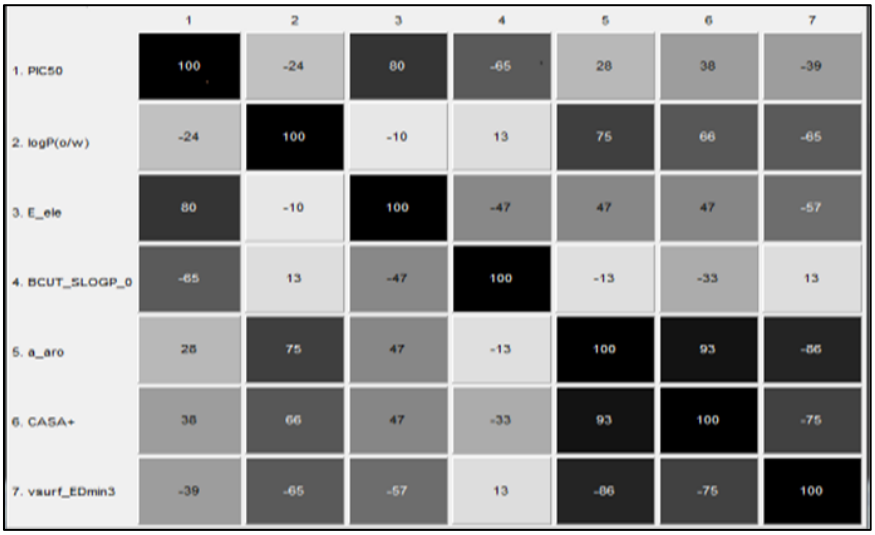

IMAGE 1: Molecular mixed (2D & 3D) descriptor correlation matrix

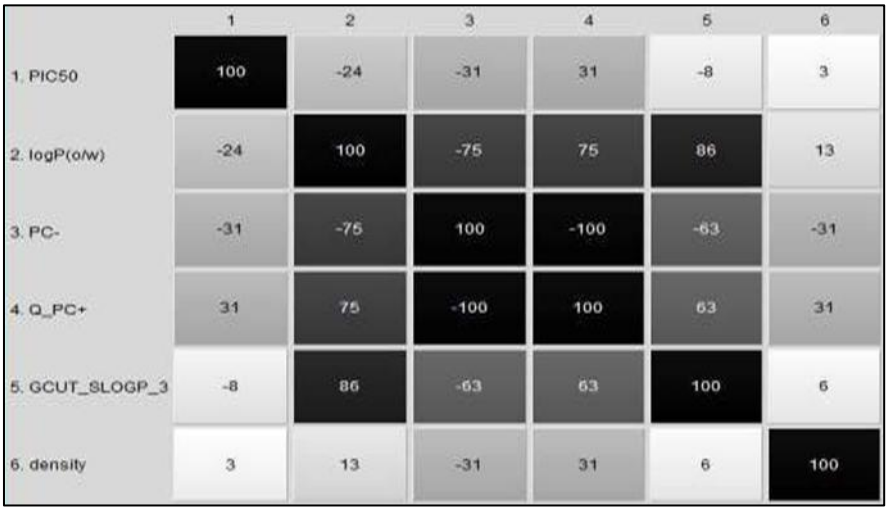

IMAGE 2: Molecular (2D) descriptor correlation matrix

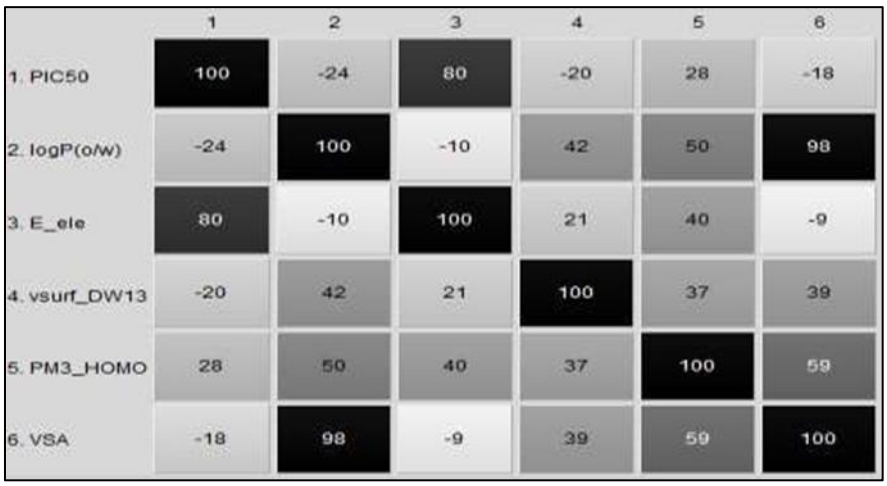

IMAGE 3: Molecular (3D) descriptor correlation matrix

The IC_{50} values in microgram per milliter (half maximal inhibitory concentration) is a quantitative measure that indicates how much of a particular drug is needed to inhibit (in vitro) a given biological process. It was converted into negative logarithmic concentration in moles (pIC_{50}). The values of pIC_{50} along with the *N*-(substituted)-9-alkyl-1-substituted-9*H*-β- carboline-3-carboxamide can be found on Table 1.

The QSAR study was performed using molecular modeling studies of compounds with Molecular Operating Environment software package (MOE, version 2015.10; Chemical Computing Group Inc.). A set of 15 compounds was used as training set for the present QSAR modeling; the remaining four was used as test set. In addition, an external test compounds have been selected randomly and used to assess the predictive power and accuracy of the resulting QSAR model.

2.1.1 Molecular descriptors

The molecular Descriptors are the numerical values associated with the chemical constitution for correlation of chemical structure with various physical properties, chemical reactivity, or biological activity (Roy *et al*, 2015; Vračko, 2016).

Total of six molecular descriptors namely Log $P_{(o/w)}$ [*Log of the octanol/water partition coefficient*], E_ele [*Electrostatic component of the potential energy*], BCUT_SLOGP_0 [*The BCUT descriptors using atomic contribution to log P (using the Wildman and Crippen Slog P method) instead of partial charge*], CASA+ [*Positive charge weighted surface area, ASA+ times max {$q_i > 0$}*], a_aro [*Number of aromatic atoms*], vsurf_EDmin3 [*3rd Lowest hydrophilic energy*], PC- [*Total negative partial charge*], Q_PC+ [*Relative positive partial charge*], GCUT_SLOGP_3 [*The GCUT descriptors using atomic contribution to logP (using the Wildman and Crippen Slog P method) instead of partial charge*], density [*Molecular mass density: Weight divided by vdw_vol (amu/Å3)*], PM3_HOMO [*The energy (eV) of the Highest Occupied Molecular Orbital calculated using the PM3 Hamiltonian [MOPAC]*], VSA [*van der Waals surface area. A polyhedral representation is used for each atom in calculating the*

surface area] and vsurf_DW3 [*Contact distances of vsurf_EWmin*] were calculated for each compound using MOE program. Calculated values of these descriptors are shown in Tables 2, 3 and 4. To select the optimum subset of proper connected, highly correlated chemical descriptors were excluded through covariance analysis using a correlation matrix (image 1, 2, and 3).

The ratio of the number of compounds to the descriptors used for the correlation is usually 5:1 (Vaidya *et al*, 2012). Thus, for the 15 compounds in the training set, only three descriptors was correlated simultaneously with their human hepatocellular carcinoma; models 1, 2, and 3. The statistical quality of the regression equations was justified by statistical parameters such as the root mean square error (RMSE), correlation coefficient (*r*), squared correlation coefficient (r^2), cross-validated [adjusted r square] (q^2), standard error of estimate (S) and F-test value (ratio between the variances of observed and calculated activities, F). Calculation of statistical parameters was carried out by using statistical program (IBM Statistics SPSS version 25).

The mixed (2D & 3D) descriptors equation:

pIC50 *= 2.24296 – [0.57073 × log P(o/w)] + [0.08413 × Q_VSA_PPOS]+ [1.41186 × std_dim2]*..(1)

Table 5. Statistical parameters used for statistical quality of model 1 of mixed (2D & 3D) descriptors

r	r2	RMSE	q2	S	F	P value
0.9810	0.9632	0.10514	0.92682	0.14855	96.089	0.0000

The (2D) descriptors equation

pIC50 = *9.83727 + [0.09608 × log P(o/w)] + [0.06326 × Q_VSA_PPOS] - [0.82343 × radius]*..(2)

Table 6. Statistical parameters used for statistical quality of model 2 of (2D) descriptors

r	r2	RMSE	q2	S	F	P value
0.9730	0.9464	0.13505	0.9019	0.1831	64.7940	0.000

The (3D) descriptors equation

pIC50 = *-1.68637- [0.88601× log P(o/w)] - [3.65753 × vsurf_EDmin2] + [0.00341 × vsurf_Wp2]*..(3)

Table 7. Statistical parameters used for statistical quality of model 3 of (3D) descriptors

r	r2	RMSE	q2	S	F	P value
0.9680	0.9368	0.12615	0.88944	0.16697	54.347	0.000

Table 8. Observed and predicted pIC50 for training set and cross validation against human hepatocellular carcinoma cell line (Bel7402) using model (1) (2D & 3D)

ID	pIC50 obs	pIC50 pred	Residuals	CV pred	Residuals
1	7.7959	7.7339	0.062	7.721	0.0749
2	7.5258	7.4609	0.0649	7.4455	0.0803
3	8.2518	8.1618	0.09	8.1261	0.1257
4	7.4737	7.5897	-0.116	7.6347	-0.161
5	7.8601	7.659	0.2011	7.5567	0.3034
6	7.5331	7.6683	-0.1352	7.7032	-0.1701
7	8.1463	8.2154	-0.0691	8.2436	-0.0973
8	6.9101	7.0672	-0.1571	7.1018	-0.1917
9	6.7595	6.6604	0.0991	6.6181	0.1414
10	6.9626	6.8659	0.0967	6.8261	0.1365
11	6.9666	6.9833	-0.0167	6.9896	-0.023
12	6.9172	6.9758	-0.0586	7.0089	-0.0917
13	7.5719	7.6158	-0.0439	7.622	-0.0501
14	6.3747	6.4906	-0.1159	6.5766	-0.2019
15	6.6289	6.5302	0.0987	6.4904	0.1385

Table 9. Predicted pIC50 values of test set using model (1) (2D & 3D)

ID	pIC50 obs	pIC50 pred	Residuals
1	7.475	7.1772	0.2978
2	7.4841	6.9966	0.4875
3	6.3788	6.8939	-0.5151
4	7.719	6.9705	0.7485

Table 10. Observed and predicted pIC50 for training set and cross validation against human hepatocellular carcinoma cell line (Bel7402) using model (2) (2D)

ID	pIC50 obs	pIC50 pred	Residuals	CV pred	Residuals
1	7.7959	7.9715	-0.3002	8.0125	-0.2166
2	7.5258	7.2495	0.2763	7.2256	0.3002
3	8.2518	8.1217	0.1301	8.0685	0.1833
4	7.4737	7.3706	0.1031	7.3444	0.1293
5	7.8601	7.9139	-0.0538	7.9552	-0.0951
6	8.1463	8.0969	0.0494	8.0775	0.0688
7	7.475	7.5227	-0.0477	7.5349	-0.0599
8	6.7595	6.8335	-0.074	6.872	-0.1125
9	6.9626	6.9545	0.0081	6.9523	0.0103
10	7.4841	7.5306	-0.0465	7.543	-0.0589
11	6.9172	6.8087	0.1085	6.7767	0.1405
12	7.5719	7.6808	-0.1089	7.7004	-0.1285
13	6.3788	6.6447	-0.2659	6.8035	-0.4247
14	6.3747	6.4369	-0.0622	6.5012	-0.1265
15	6.6289	6.4697	0.1592	6.4067	0.2222

Table 11. Predicted pIC50 values of test set using model (2) (2D)

ID	pIC50 obs	pIC50 pred	Residuals
1	7.5331	7.9466	-0.4135
2	6.9101	7.5553	-0.6452
3	6.9666	7.4978	-0.5312
4	7.719	6.6197	1.0993

Table 12. Observed and predicted pIC50 for training set and cross validation against human hepatocellular carcinoma cell line (Bel7402) using model (3) (3D)

ID	pIC50 obs	pIC50 pred	Residuals	CV pred	Residuals
1	7.7959	7.8371	-0.0412	7.8459	-0.05
2	7.5258	7.4522	0.0736	7.4453	0.0805
3	7.4737	7.4139	0.0598	7.3955	0.0782
4	7.8601	7.6953	0.1648	7.6378	0.2223
5	7.5331	7.7052	-0.1721	7.7466	-0.2135
6	8.1463	8.0581	0.0882	8.0032	0.1431
7	7.475	7.1935	0.2815	7.1315	0.3435
8	6.9101	7.0645	-0.1544	7.0967	-0.1866
9	6.9626	6.8992	0.0634	6.849	0.1136
10	6.9666	7.1074	-0.1408	7.1468	-0.1802
11	7.4841	7.5373	-0.0532	7.5477	-0.0636
12	6.9172	6.8929	0.0243	6.8877	0.0295
13	7.5719	7.7303	-0.1584	7.7742	-0.2023
14	6.3788	6.4573	-0.0785	6.5682	-0.1894
15	6.3747	6.3317	0.043	6.2868	0.0879

Table 13. Predicted pIC50 values of test set using model (3) (3D)

ID	pIC50 obs	pIC50 pred	Residuals
1	8.2518	7.7336	0.5182
2	6.7595	6.1943	0.5652
3	6.6289	6.1934	0.4355
4	7.719	6.9532	0.7658

The leave-one-out (LOO) cross-validation method (CV) was used to validate the predictive powers of the obtained models. The cross validated squared correlation coefficient (q2) was considered for the validation of these models (Tables 5, 6, 7). The developed QSAR model equation showed a relation-ship between predicted pIC50 (-Log IC50) values and chemical descriptors.

Validation of quantitative structure-activity relationship model

The QSAR models were validated to assess their prediction and robustness by internal and external validation methods (Benfenati et al, 2007). The most common used method for internal validation was cross-validation (CV). In this study we use leave-one-out (LOO) cross-validation (CV); which it's accomplished by eliminating a molecule and creating and validating the model against the individual molecules for the entire training set. Once complete, the mean was taken of all the q2 values and reported. The most vital validation is the external validation, which consists of making predictions for an independent set (test set) of compounds, which are not used in the training set. According, to the statistical results on tables 5, 6, and 7 model 1 (2d+3d) was selected to be the best model and the designed compounds activities were calculated using it (table 14). It is evident that the molecular descriptors, namely Log P(o/w) partition coefficient and E_ele are negatively correlated. In the other hand the E_ele descriptor is negatively correlated to BCUT_SLOGP_0.

The observed activities and those predicted by QSAR models 1, 2, & 3 for training sets tables 8, 10, & 12; and for test sets Tables 9, 11, & 13. It should be noted that the predicated anticancer activities by obtained QSAR models were close to those experimentally observed, indicating that these models can be safely applied for predication of more effective hits having the same skeletal framework as that of the potent anticancer compound.

2.1.3. Predict the activity of N-(2-amino-2-substitutedethyl)-9- (substituted) -6- substituted-1-substituted-9H-β-carboline-3-carboxamide compounds (A1-A50)

A set of designed N-(2-amino-2-substitutedethyl) -9-(substituted) -6- substituted -1- substituted-9H-β-carboline-3-carboxamide compounds (M1- M50) were sketched using ACD/lab free software program. These compounds were not used in the developed QSAR model, but sketched to predict their anticancer activity against Bel7402 cell line by using developed QSAR model (Equation 1). The predicted activity along with the sketched structures was listed in Table 14.

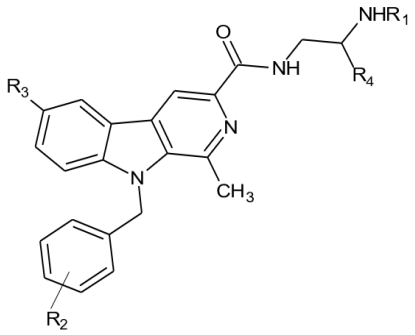

Table 14: Structures of designed N-(2-amino-2-substitutedethyl)-9-(substituted)-6- substituted-1-substituted-9H-β-carboline-3-carboxamide derivatives with their predicted pIC50 values against human hepatocellular carcinoma cell line (Bel7402)

ID	R1	R2	R3	R4	pIC50 Pre
M1	H	p-OCHO	H	H	7.7833
M2	p-CN	H	H	H	7.2798
M3	p-SO2CF3-C6H4	H	H	H	10.9106
M4	p-NO2-C6H4	H	H	H	7.4559
M5	p-SO2Cl-C6H4	H	H	H	7.7229
M6	p-COOCH3-C6H4	H	H	H	6.8604
M7	p-CONH2-C6H4	H	H	H	6.0086
M8	H	H	H	p-NH2-C6H4	6.9273
M9	H	H	H	p-OH-C6H4	7.1461
M10	H	H	H	p-OCH3-C6H4	7.2958
M11	H	H	H	p-NO2-C6H4	8.1531
M12	H	H	H	p-SO2H-C6H4	7.3447
M13	H	H	H	p-NHCOCH3-C6H4	6.5846
M14	H	H	H	p-OCHO-C6H4	7.2372
M15	H	H	H	p-SO2CF3-C6H4	11.2804
M16	H	H	H	p-CHO-C6H4	7.8071

M17	H	H	H	p-CONH2-C6H4	6.677
M18	H	H	H	p-COOH-C6H4	6.4749
M19	H	H	H	p-CF3-C6H4	8.145
M20	H	p-NH2	H	H	7.5443
M21	H	m-OH	H	H	7.683
M22	H	m-Cl	H	H	7.9718
M23	H	m-COOC2H5	H	H	7.7799
M24	H	p-NO2	H	H	8.777
M25	H	p-OCOCH3	H	H	7.9308
M26	H	p-SO3H	H	H	6.8149
M27	H	p-OCHO	H	H	7.7833
M28	H	p-NHCHO	H	H	6.9951
M29	H	p-SO2Cl	H	H	8.8612
M30	H	p-SO2CF3	H	H	11.6455
M31	H	p-CN	H	H	8.4434
M32	H	p-CF3	H	H	8.5744
M33	H	p-CHO	H	H	8.3072
M34	H	p-COCH3	H	H	8.3008
M35	H	p-COOCH3	H	H	7.9108
M36	H	p-COOC2H5	H	H	7.8928
M37	H	o-SH	H	H	7.4798
M38	H	o-Cl	H	H	7.5365
M39	H	o-CONH2	H	H	6.7033
M40	H	H	0	H	7.2667
M41	H	H	-Cl	H	7.6558
M42	H	H	0	H	8.4059
M43	H	H	-OCOCH3	H	7.661
M44	H	H	-SO2CF3	H	11.6173
M45	H	H	-COOC6H5	H	7.9987
M46	H	H	-COOC2H5	H	7.7853
M47	H	H	-COOCH3	H	7.6676
M48	H	H	-COCH3	H	8.084
M49	H	H	-CHO	H	8.1012
M50	H	H	-(CH2)3NH2	H	8.1435

2.1 Molecular docking

Docking is a computational chemistry technique can be used to predict the binding of drug-target complexes, as well as the conformation of the ligand upon binding to a protein target. The binding free energy of target-drug interactions establishes the affinity of an association and the conditions for forming a complex. Molecular docking study was carried out in order to elucidate which of the designed *N*-(2-amino-2-substitutedethyl)-9- (substituted) -6- substituted -1- substituted- 9*H*-β-carboline-3-carboxamide derivatives (A_1-A_{50}) has the best binding affinity against the hepatocellular carcinoma protein (Topoisomerase II). The structure of Topoisomerase II used in the study was obtained from Protein Data Bank with PDB code 3QX3. The structures of the designed compounds (1-50) were prepared and saved on database files (mdb) and the pocket of 3QX3 protein was isolated. The binding score (S) of the complexes and amino acid interactions are reported in Table 15. Also, the structures of the synthesized compounds (1-19) were prepared and saved on database files (mdb) and docked into the isolated pocket of 3QX3 protein. The binding score (S) of the complexes and amino acid interactions are reported in Table 14.

Table 14: Binding scores and amino acid interactions of the docked *N*-(substituted)-9- alkyl-1-substituted-9*H*-β-carboline-3-carboxamide derivatives reported by (Guan *et al*, 2006) on the active site of 3QX3

ID	S (kcal/mol)	rmsd_refine	Amino acid interaction	Type of interaction	Length (Å)
1	-6.813	1.1834	Mg	Metal bond	-
			Glu (A477)	Hydrogen bond	2.13
			DG (C13)	π-cation interaction	-
2	-7.6631	0.7401	Mg	Metal bond	
			Lys (A505)	π-cation interaction	-
			His (A775)	Hydrogen bond	2.49
			His (A775)	π-cation interaction	-
3	-9.0001	1.4509	Mg	Metal bond	-
			Arg (A945)	Hydrogen bond	2.24
4	-7.4874	1.9292	Arg (B503)	π-cation interaction	-
			Arg (B503)	π-cation interaction	-

			Asp (B449)	Hydrogen bond	1.87
5	-6.2708	1.3967	Asp (A479)	Hydrogen bond	2.16
			DG (B13)	π-cation interaction	-
6	-6.3733	1.5824	Lys (A456)	Hydrogen bond	2.33
			Lys (A456)	Hydrogen bond	2.02
7	-7.1239	1.6579	DT (C9)	π-cation interaction	-
			DG (B13)	π-cation interaction	-
8	-6.6941	1.1741	Asp (A479)	Hydrogen bond	1.99
			DG (B13)	π-cation interaction	-
9	-7.5317	1.0419	Mg	Metal bond	-
			Gly (A504)	π-cation interaction	-
10	-7.1758	1.403	Asp (A479)	Hydrogen bond	2.25
11	-7.3272	1.2462	DG (B13)	Hydrogen bond	2.53
			DG (B13)	Hydrogen bond	1.81
12	-6.2037	1.3901	Arg (A503)	π-cation interaction	-
			DG (B13)	π-cation interaction	-
			DA (B12)	Hydrogen bond	2.33
13	-6.4048	0.544	Asp (A479)	Hydrogen bond	2.42
			Glu (A477)	Hydrogen bond	2.27
			Arg (A503)	π-cation interaction	-
14	-6.7866	1.5264	Mg	Metal bond	-
			DT (C9)	π-cation interaction	-
15	-7.4857	1.9435	Mg	Metal bond	-
			Met (A782)	π-cation interaction	-
16	-7.9899	1.0789	DG (B13)	π-cation interaction	-
17	-7.4528	1.5275	DA (B12)	π-cation interaction	-
			DA (B12)	π-cation interaction	-
			DT (C9)	Hydrogen bond	1.9
18	-7.7224	1.7243	Mg	Metal bond	-
			Asp (A479)	Hydrogen bond	2.14
19	-7.566	1.5747	DG (B12)	π-cation interaction	-
			Arg (A503)	π-cation interaction	-
			Arg (A503)	π-cation interaction	-

Table 15: Binding scores and amino acid interactions of the docked *N*-(2-amino-2- substitutedethyl) -9- (substituted) -6-substituted -1- substituted -9*H*- β-carboline- 3carboxamide compounds (M1-M50) on the active site of 3QX3

ID	S (kcal/mol)	rmsd_refine	Amino acid interaction	Type of interaction	Length (Å)
M1	-7.6021	1.7196	Gln(A778)	Hydrogen bond	2.19
			Lys(A505)	Hydrogen bond	2.08
			DG(B13)	Hydrogen bond	2.12
			DC(B11)	Hydrogen bond	2.31
			DT(C9)	Hydrogen bond	2.23
			DT(C9)	π-cation interaction	-
			DA(B12)	π-cation interaction	-
M2	-8.0813	1.4433	Lys (A505)	Hydrogen bond	2.53
			Arg (503)	π-cation interaction	-
			DG (B13)	π-cation interaction	-
M3	-8.9707	1.6519	Gln (A778)	Hydrogen bond	2.49
			DG (B13)	π-cation interaction	-
M4	-7.8473	1.8592	Met (A782)	Hydrogen bond	2.86
			Gly (A478)	π-cation interaction	-
M5	-7.5805	1.5672	Asp (A479)	Hydrogen bond	2.09
			Arg (A503)	Hydrogen bond	2.27
M6	-8.8903	1.9298	Mg	Metal bond	2.07
			DT (C9) DG (B13)	π-cation interaction π-cation interaction	-
					-
M7	-8.5667	1.7211	Gly (A813)	Hydrogen bond	2.44
			Met (A782)	π-cation interaction	-
			DT (C9)	π-cation interaction	-
			DG (B13)	π-cation interaction	-
M8	-9.0235	1.4248	Mg	Metal bond	2.46
			DT (C9)	π-cation interaction	-
			DT (C9)	π-cation interaction	-
M9	-7.6248	1.5563	Lys (A505)	Hydrogen bond	2.28
			DT (C9)	π-cation interaction	-

			DG (B13)	π-cation interaction	-
M10	-8.3139	1.861	Asp (B479)	Hydrogen bond	1.86
			Arg (B503)	π-cation interaction	-
			Arg (B503)	π-cation interaction	-
M11	-8.2617	1.6121	Mg	Metal bond	2.3
			Glu (B477)	Hydrogen bond	2.32
			DG (C13)	π-cation interaction	-
			DT (D9)	π-cation interaction	-
M12	-9.7602	1.9339	Mg	Metal bond	2.1
			Mg	Metal bond	2.22
			Arg (B503)	π-cation interaction	-
			DA (C12)	π-cation interaction	-
M13	-8.4651	1.5623	Asp (A479)	Hydrogen bond	1.95
			Ala (A481)	Hydrogen bond	2.48
			DT (C9)	Hydrogen bond	2.21
M14	-9.1305	1.5549	Mg	Metal bond	2.22
			Glu (B477)	Hydrogen bond	2.1
			Glu (B477)	Hydrogen bond	2.28
			DT (D9)	π-cation interaction	-
			DT (D9)	π-cation interaction	-
M15	-7.6391	1.3718	Lys (A505)	Hydrogen bond	2.29
			DG (C13)	π-cation interaction	-
			DG (C13)	π-cation interaction	-
M16	-8.1281	1.3826	Mg	Metal bond	2.04
			Met(A782)	π-cation interaction	-
			Met(A782)	π-cation interaction	-
M17	-8.5132	1.5815	Mg	Metal bond	2.08
			Ser(A480)	Hydrogen bond	2.43
			DG(D13)	π-cation interaction	-
M18	-8.6297	1.629	DG(C13)	Hydrogen bond	2.13
			DC(C14)	Hydrogen bond	2.45
			DA(C12)	π-cation interaction	-
M19	-9.1456	1.4879	Mg	Metal bond	2.18
			Arg (A503)	π-cation interaction	-
			DG (D13)	π-cation interaction	-
			DT (C9)	π-cation interaction	-
			DT (C9)	π-cation interaction	-
M20	-7.1893	0.6664	Ser (A480)	Hydrogen bond	2.41
			Arg (A503)	π-cation interaction	-
			Arg (A503)	π-cation interaction	-
			DT (C9)	π-cation interaction	-
M21	7.6792	1.3555	Asp (A479)	Hydrogen bond	1.92
			DG (C13)	π-cation interaction	-
M22	-7.6508	0.9547	Mg	Metal bond	2.17
			Gly (A776)	Hydrogen bond	2.51
M23	-9.0518	1.5741	Mg	Metal bond	2.23
			DT (B9)	π-cation interaction	-
M24	-7.7075	0.8914	Asp (A479)	Hydrogen bond	2.59
			DA (C12)	π-cation interaction	-
M25	-8.0211	1.2013	Arg (A503)	π-cation interaction	-
			Arg (A503)	π-cation interaction	-
			DA (B12)	Hydrogen bond	2.49
M26	-7.8108	1.692	Mg	Metal bond	2.05
			His (A775)	Hydrogen bond	2.1
			DG (B13)	π-cation interaction	-
M27	-7.6021	1.7196	Gln (A778)	Hydrogen bond	2.19
			Lys (A505)	Hydrogen bond	2.08
			DG (B13)	Hydrogen bond	2.12
			DC (B11)	Hydrogen bond	2.31
			DT (C9)	Hydrogen bond	2.23
			DT (C9)	π-cation interaction	-
			DA (B12)	π-cation interaction	-
M28	-8.347	1.372	Asp (A479)	Hydrogen bond	2.11
			Gln (A778)	Hydrogen bond	2.3
			DG (B13)	π-cation interaction	-
M29	-7.5899	0.6037	Lys (A505)	Hydrogen bond	2.2
			Arg (A729)	Hydrogen bond	2.38
			DT (B15)	Hydrogen bond	2.21
			DG (B13)	π-cation interaction	-

			DA (B12)	π-cation interaction	-
M30	-7.9299	1.73	Asp (B479)	Hydrogen bond	2.05
			Arg (B503)	π-cation interaction	-
M31	-8.5042	1.542	Mg	Metal bond	2.2
			Glu (A477)	Hydrogen bond	2.38
			DG (B13)	π-cation interaction	-
M32	-9.0674	1.4452	Mg	Metal bond	2.18
			Mg	Metal bond	2.03
M33	-8.6951	0.8552	Mg	Metal bond	2.17
			Mg	Metal bond	2.2
			DT (B15)	Hydrogen bond	2.41
M34	-7.8056	0.9364	Asp (A479)	Hydrogen bond	2.18
			Ser (A480)	Hydrogen bond	2.39
			Arg (A503)	π-cation interaction	-
			Arg (A503	π-cation interaction	-
M35	-8.6137	1.6873	Mg	Metal bond	2.16
			Mg	Metal bond	2.03
			DT (C9)	π-cation interaction	-
M36	-8.6065	1.7365	Asp (B479)	Hydrogen bond	1.92
			DG (C13)	π-cation interaction	-
M37	-7.4644	1.8205	Lys (A456)	Hydrogen bond	2.15
			Arg (A503)	π-cation interaction	-
			Arg (A503)	π-cation interaction	-
			Arg (A503)	Hydrogen bond	2.66
			DG (C10)	Hydrogen bond	2.33
M38	-7.4372	1.4335	Lys (A456)	Hydrogen bond	2.25
			Arg (A503)	π-cation interaction	-
			Arg (A503)	π-cation interaction	-
			DT (C9)	π-cation interaction	-
M39	-7.5691	1.312	Mg	Metal bond	2.13
			Glu (A477)	Hydrogen bond	2.16
			Ala (A779)	π-cation interaction	-
M40	-7.2133	0.966	Gln (A778)	Hydrogen bond	2.39
			DG (B13)	π-cation interaction	-
			DT (C9)	π-cation interaction	-
			DA (B12)	π-cation interaction	-
M41	-7.4907	0.8225	Gln (A778)	Hydrogen bond	2.19
			DT (C9)	π-cation interaction	-
			DG (B13)	π-cation interaction	-
M42	-8.0125	1.6516	Asp (A479)	Hydrogen bond	2.07
			Lys (A456)	Hydrogen bond	2.31
			Arg (A503)	π-cation interaction	-
			DA (B12)	π-cation interaction	-
M43	-7.3846	1.2082	Mg	Metal bond	2.07
			Met (A782)	Hydrogen bond	2.65
			Ala (A779)	π-cation interaction	-
			DT (C9)	π-cation interaction	-
M44	-7.6984	1.7349	Lys (B505)	Hydrogen bond	2.42
			DG (B13)	Hydrogen bond	2.38
			DG (B13)	Hydrogen bond	2.5
M45	-8.9628	1.6554	Asp (A479)	Hydrogen bond	2.1
			Lys (B456)	Hydrogen bond	2.17
			Arg (B503)	Hydrogen bond	2.31
			DG (D10)	π-cation interaction	-
M46	-8.3118	1.6986	Asp (A479)	Hydrogen bond	1.9
			Arg (A503)	π-cation interaction	-
			Arg (A503)	π-cation interaction	-
M47	-8.3309	1.4339	Asp (A479)	Hydrogen bond	1.9
			Arg (B503)	π-cation interaction	-
			Arg (B503)	π-cation interaction	-
M48	-9.0594	1.2789	Mg	Metal bond	2.22
			Mg	Metal bond	2.04
M49	-7.5919	1.1654	Gln (A778)	Hydrogen bond	2.41
			DT (C9)	π-cation interaction	-
			DG (B13)	π-cation interaction	-
			DA (B12)	π-cation interaction	-
M50	-7.6436	1.2282	Lys (B505)	Hydrogen bond	2.06
			DC (C14)	Hydrogen bond	2.32
			DT (D9)	π-cation interaction	-

3. Results and discussion

3.1 QSAR studies

In order to develop accurate, robust and efficient QSAR models to predict leukemia anticancer activity of *N*-(substituted)-9-alkyl-1-substituted-9*H*-β- carboline-3-carboxamide derivatives, a small subset of descriptors which represent the total set of descriptors has been identified through this work.

The developed QSAR models 1, 2, & 3 showed that the squared correlation coefficient (R^2 = 0.9760, 0.9461, & 0.9439) and cross validation R square (Q^2= 0.9030, 0.8997, & 0.91108), the difference between the R^2 cross validation R square value is less than 0.3. The root means square error (RMSE = 0.1281, 0.1333, & 0.1380) was less than 0.3 (RMSE ≤ 0.3) showed good predictive model, all other statistical parameters calculated to justified the statistical quality of models were in acceptable rang tables 5, 6, and 7.

Leave-One-Out (LOO) method of cross-validation (CV) was performed to assist the predictively and robustness of the model when (Q^2 > 0.5) was an ultimate proof of the high predictive power of the QSAR model.

Figures 1, 2 and 3 **(model 1)** show the corresponding scatter plots of the pIC_{50} observed versus pIC_{50} predicted values for the training set, cross validation and test set compounds against hepatocellular carcinoma cell line (Bel7402), respectively.

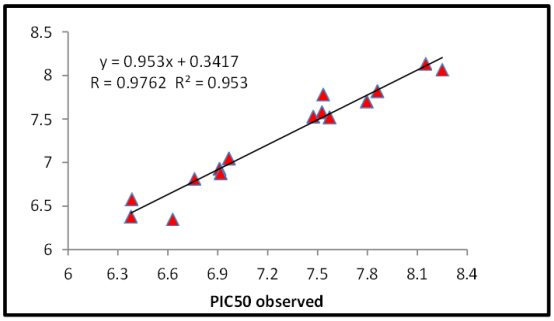

Figure 1: pIC50 Predicted versus pIC50 observed values of training set against hepatocellular carcinoma cell line (Bel7402)

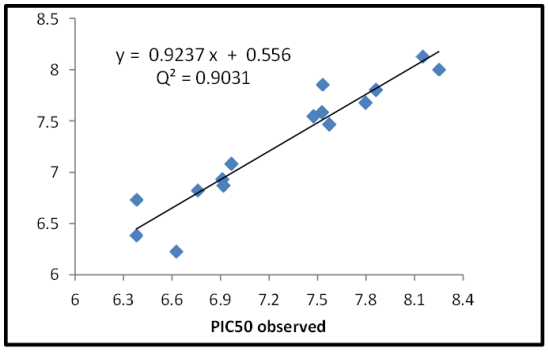

Figure 2: pIC50 Cross-Validation Predicted values versus pIC50 observed values of training set against hepatocellular carcinoma cell line (Bel7402)

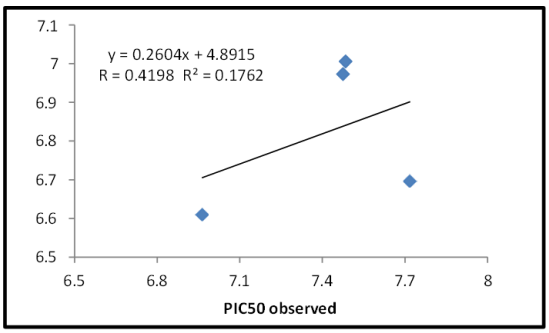

Figure 3: pIC50 Predicted values versus pIC50 observed values of test set against hepatocellular carcinoma cell line (Bel7402)

3.2 Docking study

The designed *N*-(2-amino-2-substitutedethyl)-9-(substituted)-6-substituted-1- substituted-9*H*-β-carboline-3-carboxamide compounds (M_1-M_{50}) were docked using MOE docking tool into the optimized target protein (Topoisomerase II) binding site (protein pocket). All the molecules were found to exhibit significant docking scores. The results generated by the *in-silico* analysis are presented in Table 15.

All docked compounds exhibited an analogous conformation and positions in an active binding site of 3QX3 protein structure which may provide an understanding of their effect as anticancer agents. The binding affinity and the scoring function were used to give a good approximation of the binding free energy between a ligand and a receptor. The values of docking score for designed compounds range from -9.7602 to -7.1893 kcal/mol as listed in Table 8. In the other hand, the binding affinity values for synthesized compounds range from -9.0001 to -6.2037 kcal/mol as listed in table 14.

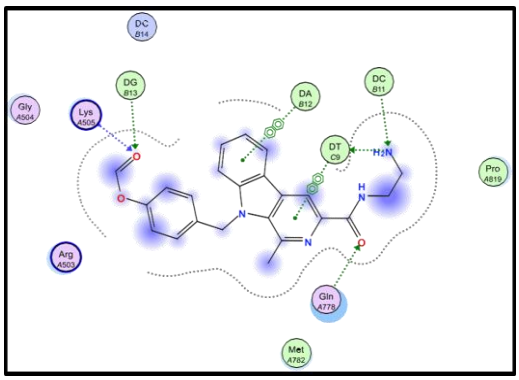

Figure 4: 2D molecular docking model of compounds M1 with 3QX3

All ligands docking pose were analyzed, they inhibit topoisomerase II by intercalating the DNA and thereby inhibiting topoisomerase II in the process. Compound M_{12} and M_{19} are appeared as the highest binding score drugs, - 9.7602 and -9.1456 kcal/mol respectively. Compound M_1 with binding score - 7.6021 appear as most active

topoisomerase II inhibitor studied Here; by showing a number of bonds as the same as that for the lead compound and some new added bonds. Compound M_1 bound to the receptor through five hydrogen bonding interactions as following: Gln_778 (2.19 A°), Lys_505 (2.08 A°), DG13 (2.12 A°), DC11 (2.31 A°) and DT9 (2.23 A°) and and two π- bonds interactions: DT9 and DA12 (Figures 4 and 5).

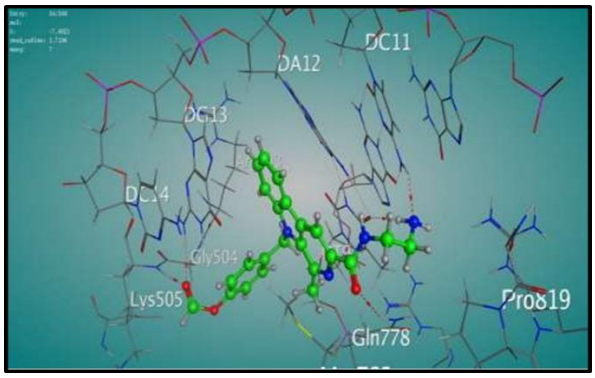

Figure 5: 3D model of the interaction between compounds M1 with 3QX3

Conclusion

In the current study, the QSAR model has been built based on theoretical molecular descriptors of N-(substituted)-9-alkyl-1-substituted-9H-β- carboline-3-carboxamide (1-19). It used for design new N-(2-amino-2-substitutedethyl) -9- (substituted) -6- substituted-1 substituted-9H-β-carboline- 3-carboxamide compounds (M1-M50) which were used as drug candidates for hepatocellular carcinoma by targeting topoisomerase II protein. The molecular docking study of (M1-M50) compounds has been done for the better understanding of the ligand-receptor interaction and the results confirmed that these compounds were a potential inhibitor of topoisomerase II protein. As a continuation of this work, we plan further modifications of these promising structures (M12 and M19) and other pharmacological experiments, in an in vivo model, as well.

References

[1] Abdolmaleki, A., Ghasemi, F., and Ghasemi, J. B. (2017). Computer- aided drug design to explore cyclodextrin therapeutics and biomedical applications. Chemical Biology and Drug Design,89, 257-268.

[2] Almaqwashi, A. A., Paramanathan, T., Rouzina, I., and Williams, M.C. (2016). Mechanisms of small molecule-DNA interactions probed by single-molecule force spectroscopy. Nucleic Acids Research. 44, 3971 3988

[3] Anwanwan, D., Singh, S. K., Singh, S., Saikam, V., Singh, R. (2020). Challenges in liver cancer and possible treatment approaches. Biochimica et Biophysica Acta - Reviews on Cancer, 1873, 188314- 188338.

[4] Benfenati, E., Chrétien, J. R., Gini, G., Piclin, N., Pintore, M., and Roncaglioni, A. (2007). Validation of the models. Quantitative Structure-Activity Relationships (QSAR) for Pesticide Regulatory Purposes. Elsevier B.V., pp.185-199.

[5] El-Miligy, M.M., Rida, S. M., Ashour, F. A., Badr, M. H., El-Bassiony, E. M., El-Demellawy, M. A., and Omar, A. M. (2018). Dual inhibitors of hepatitis C virus and hepatocellular carcinoma: Design, synthesis and docking studies. Future Science OA, 4(1), FSO252.

[6] Ferlay, J., Ervik, M., Lam, F., Colombet, M., Mery, L., and Piñeros, M. (2020). Global Cancer Observatory: Cancer Today. Lyon: International Agency for Research on Cancer. World Health Organization (WHO), 419, 2. (https://gco.iarc.fr/today, accessed February 2021).

[7] Fischer, E. (1894). Einfluss der Configuration auf die Wirkung der Enzyme. Berichte der deutschen chemischen Gesellschaft, 27(3), 2985- 2993.

[8] Guan, H., Chen, H., Peng, W., Ma, Y., Cao, R., Liu, Xiaodong., and Anlong Xu. (2006). Design of β-carboline derivatives as DNA-targeting antitumor agents. European Journal of Medicinal Chemistry, 41, 1167-1179.

[9] Li, J., Luo, D., Wen, T., Liu, Q., and Mo, Z. (2021). Representative feature selection of molecular descriptors in QSAR modeling. Journal of Molecular Structure, 1244, 131249-131257.

[10] Li, M., Huang, W., Jie, F., Wang, M., Zhong, Y., Chen, Q., & Lu, B. (2019). Discovery of Keap1-Nrf2 small-molecule inhibitors from phytochemicals based on molecular docking. Food and Chemical Toxicology, 133, 110758.

[11] Llovet, J. M., Kelley, R. K.,Villanueva, A., Singal, A. G., Pikarsky, E., Roayaie, S., Lencioni, R., Koike, K., Zucman-Rossi, J., and Finn, R. (2021). Hepatocellular carcinoma. Nature Reviews Disease Primers, 7(1), 6-34

[12] Man, S., Luo, C., Yan, M., Zhao, G., Ma, L., and Gao, W. (2012). Treatment for liver cancer: From sorafenib to natural products. European Journal of Medicinal Chemistry. 224, 113690

[13] Martinez, M. J., Razuc, M., and Ponzoni, I. (2019). MoDeSuS: A machine learning tool for selection of molecular descriptors in qsar studies applied to molecular informatics. BioMed Research International, 2019, 2905203–2905214.

[14] Omran, D. M., Ghaly, M. A., El-Messery, S. M., Badria, F. A., Abdel- L. Ehab., and Shehata, I. A. (2019). Targeting hepatocellular carcinoma: Synthesis of new pyrazole-based derivatives, biological evaluation, DNA binding, and molecular modeling studies. Bioorganic Chemistry, 88, 102917.

[15] Roy, K., Kar, S., and Das, R. N. (2015). Chapter2: Chemical Information and Descriptors. Understanding the Basics of QSAR for Applications in Pharmaceutical Sciences and Risk Assessment: Academic Press,pp,47-80.

[16] Suganya, V., and Anuradha, V. (2019). In silico molecular docking of astaxanthin and sorafenib with different apoptotic proteins involved in hepatocellular carcinoma. Biocatalysis and Agricultural Biotechnology, 19, 101076-101083.

[17] Taïbi, N., Al-balas, Q. A., Bekari, N., Talhi, O., Al Jabal, G. A., Benali, Y., Ameraoui, R., Hadjadj, M., Taïbi, A., Boutaiba, Z. M., Abou-Mustapha, M., Khammar, F., Dergal, F., Hassaine, R., Boukenna, L., Bacharia, K., Soares Silva, A. M. (2019). Design, molecular docking, in vitro, and in vivo studies of new quinazolin-4(3H)-ones as VEGFR-2 inhibitors with potential activity against hepatocellular carcinoma. Bioorganic Chemistry, 19, 12882-12894.

[18] Vaidya, S. S., Vinaya, H., and Mahajan, S. S. (2012). Microwave-assisted synthesis, pharmacological evaluation, and QSAR studies of 1,3-diaryl-2-propen-1-ones. Medicinal Chemistry Research, 21(12), 4311–4323.

[19] Villanueva, A. (2019). Hepatocellular carcinoma. New England Journal of Medicine. 380, 1450–1462.

[20] Vračko, M. (2016). Chapter 10: Mathematical (Structural) Descriptors in QSAR: Applications in Drug Design and Environmental Toxicology. Advances in Mathematical Chemistry and Applications: Bentham Science Publishers,pp, 222-250.